Electronic Supplementary Material (ESI) for Nanoscale.

Electronic Supplementary Information

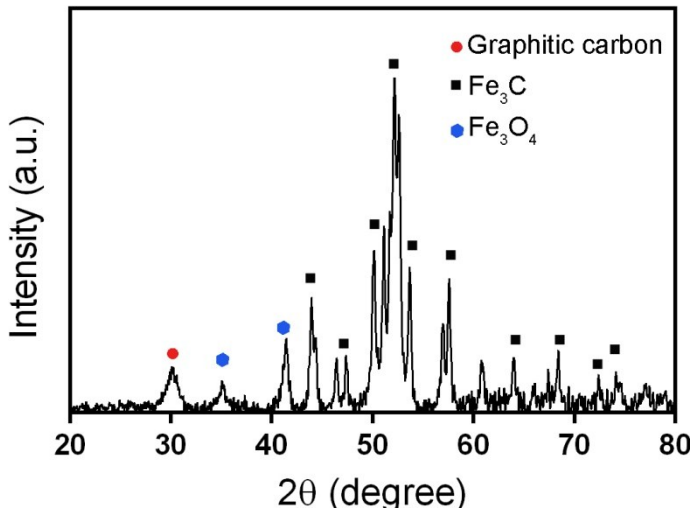

Fig. S1 XRD pattern of Fe_3C/Fe_3O_4@GC nanocomposite.

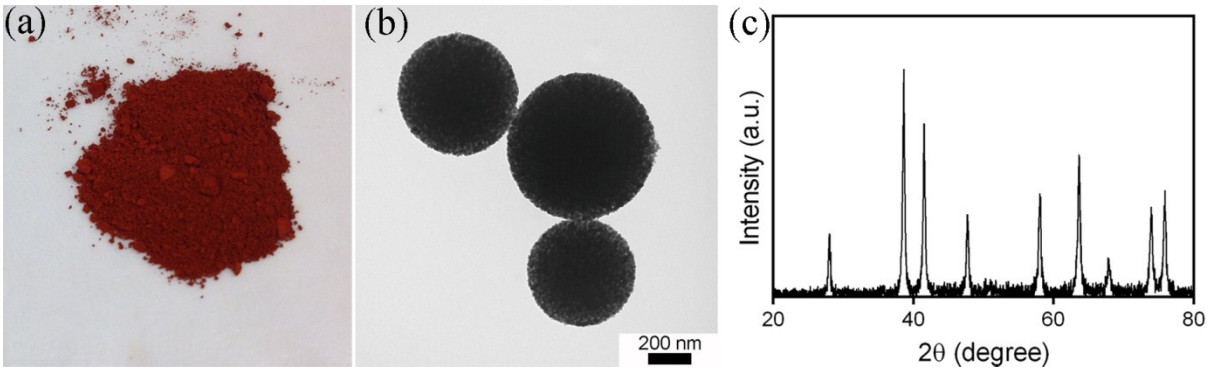

Fig. S2 Digital image (a), TEM image (b) and XRD pattern (c) of the sample carbonized at 500 ºC and then oxidized at 350 ºC.

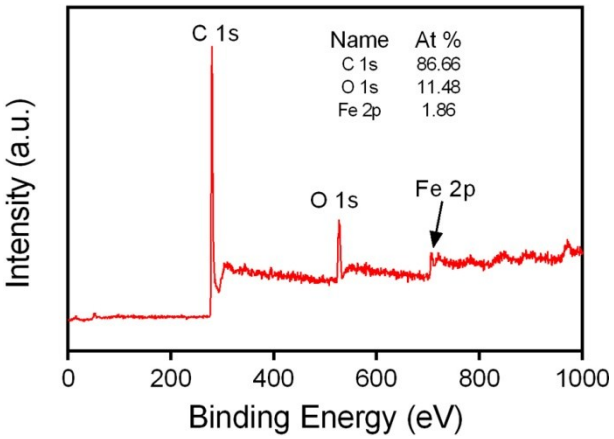

Fig. S3 XPS spectrum of α-Fe_2O_3@GC.

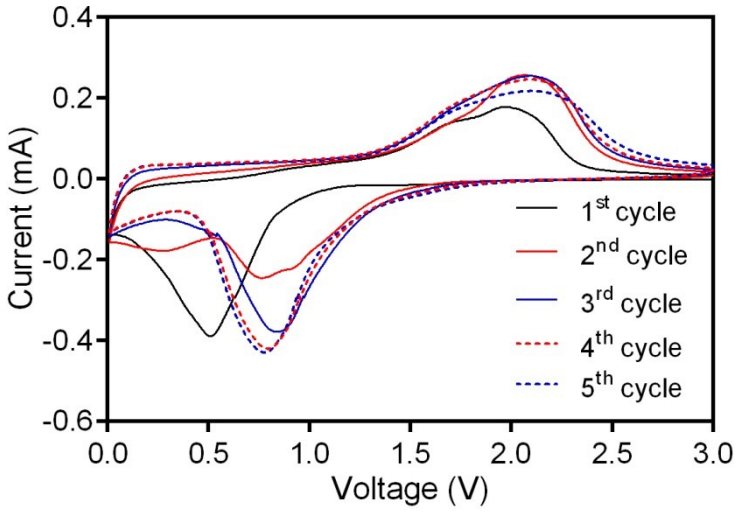

Fig. S4 Cyclic voltammogram (CV) curves of α-Fe_2O_3@GC at a scan rate of 0.1 mV.

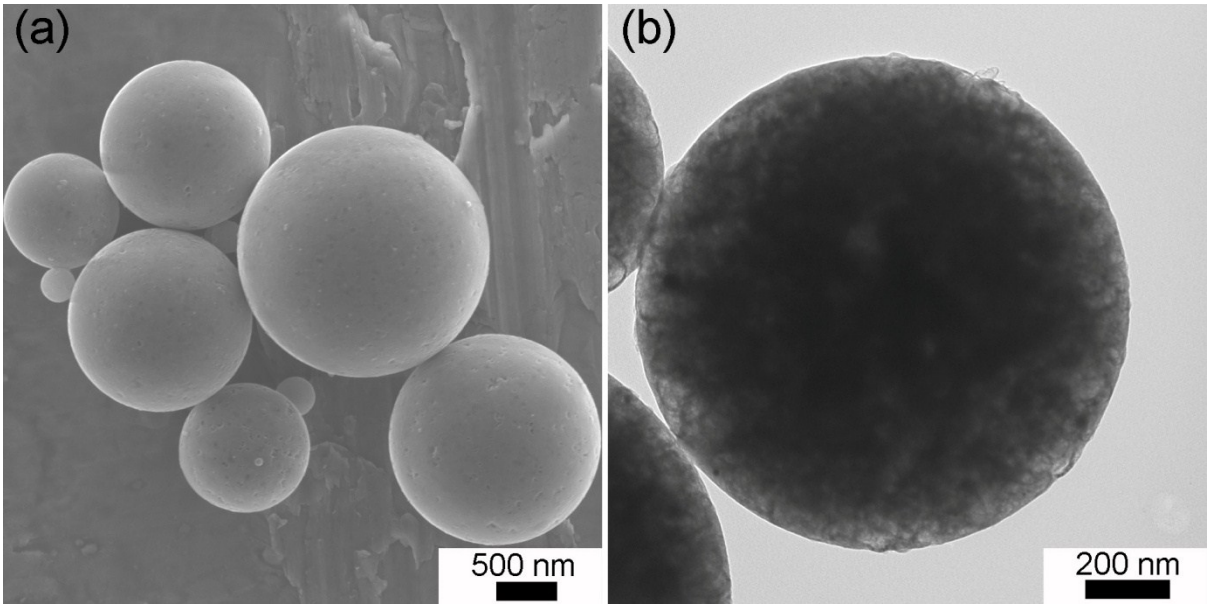

Fig. S5 SEM (a) and TEM (b) images of bare graphitic carbon microspheres prepared by eniminating α-Fe_2O_3 from the α-Fe_2O_3@GC.

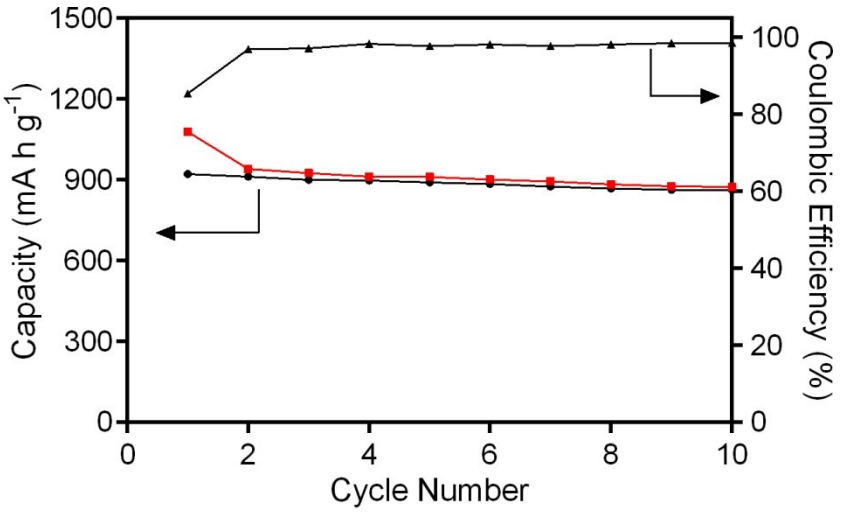

Fig. S6 Initial Coulombic efficiency of α-Fe_2O_3@GC by applying a prelithiation strategy.

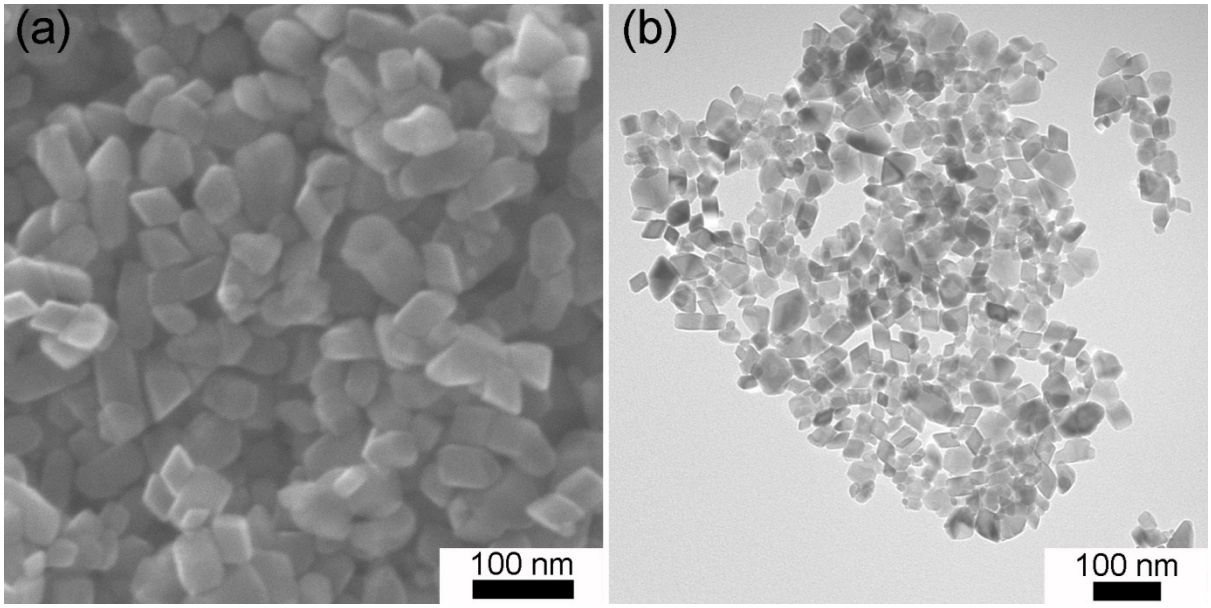

Fig. S7 SEM (a) and TEM (b) images of prestine α-Fe_2O_3 nanoparticles.

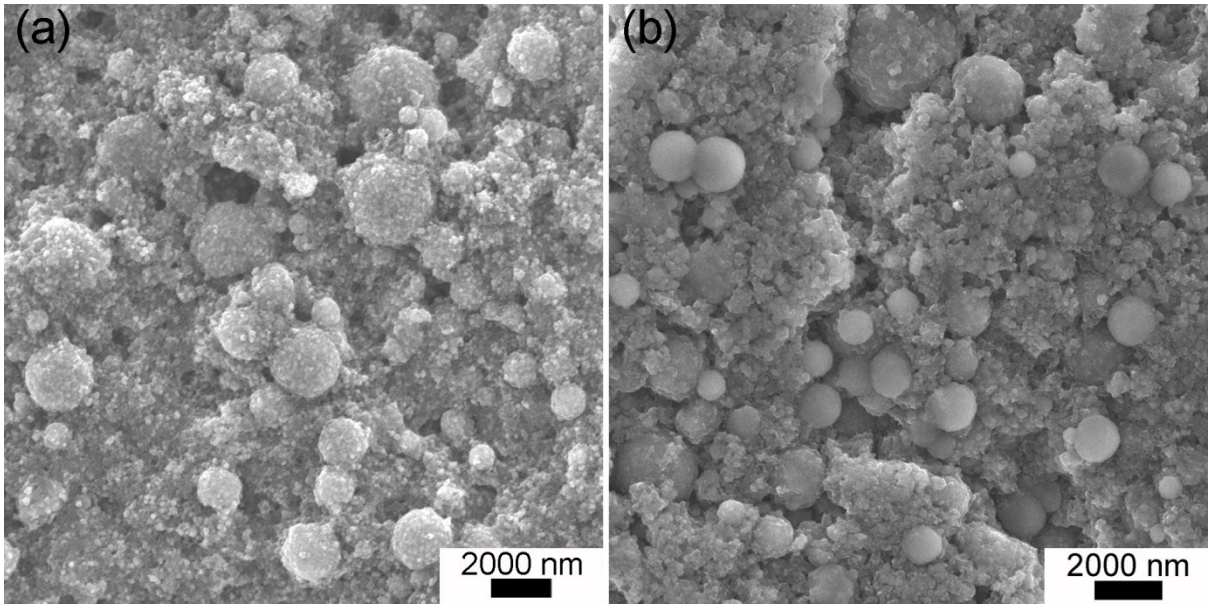

Fig. S8 SEM images of electrode before cycling (a) and after 100 cycles at 400 mA g^{-1} (b).

Table. S1 A comparison of the electrochemical performance of α-Fe_2O_3 based anodes from literature.

Type of materials	Current /mA g^{-1}	Cycles	Reversible capacity (mA h g^{-1})	References
Mesoporous α-Fe_2O_3	200	50	911	S1
Hollow α-Fe_2O_3	200	100	710	S2
Fe_2O_3 Microboxes	200	30	945	S3
Multi-Shelled α-Fe_2O_3	400	50	1000	S4
Multi-Shelled α-Fe_2O_3	300	80	848	S5

References

S1 X. Xu, R. Cao, S. Jeong and J. Cho, *Nano Lett.*, 2012, **12**, 4988-4991.
S2 B. Wang, J. S. Chen, H. B. Wu, Z. Y. Wang and X. W. Lou, *J. Am. Chem. Soc.*, 2011, **133**, 17146-17148.
S3 L. Zhang, H. B. Wu, S. Madhavi, H. H. Hng and X. W. Lou, *J. Am. Chem. Soc.*, 2012, **134**, 17388-17391.
S4 L. Zhou, H. Y. Xu, H. W. Zhang, J. Yang, S. B. Hartono, K. Qian, J. Zou and C. Z. Yu, *Chem. Commun.*, 2013, **49**, 8695-8697.
S5 M. Y. Son, Y. J. Hong, J. K. Lee and Y. C. Kang, *Nanoscale*, 2013, **5**, 11592-11597.